GEOPHYSICAL RESEARCH LETTERS, VOL. 22, NO. 16, PAGES 2249-2252, AUGUST 15, 1995

A broadband P wave analysis of the large deep Fiji Island and Bolivia earthquakes of 1994

Saskia Goes and Jeroen Ritsema
Institute of Tectonics and W. M. Keck Seismological Laboratory, University of California, Santa Cruz

Abstract. The complex broadband *P*-wave displacement recordings of the 570 km deep March 9, 1994, M_w 7.6 Fiji Island and the 660 km deep June 9, 1994, M_w 8.2 Bolivia earthquakes are analyzed to estimate the spatial and temporal characteristics of their ruptures. We model relative arrival times and amplitudes of coherent subevents in *P* waveforms, and perform waveform analyses. We resolve: (1) short rupture durations relative to their seismic moments, 12 and 40 s for the Fiji and Bolivia earthquakes, respectively; (2) small areas of main moment release, for both earthquakes 30x40 km^2; (3) high stress drops compared to shallow earthquakes, with the stress drop of the Bolivia event (283 MPa) being significantly higher than the stress drop of the Fiji event (26 MPa); (4) small changes in mechanism (up to 10° changes in fault plane orientation); and (5) a steeply dipping rupture plane for the Fiji earthquake, and a shallowly dipping rupture plane for the Bolivia earthquake. Details of the ruptures are difficult to resolve using teleseismic P waveforms.

Introduction

Few seismological characteristics distinguish deep-focus earthquakes (depth >300 km) from shallow, frictional sliding earthquakes. Deep earthquakes tend to have relatively high stress drops, short rupture durations and few aftershocks (see *Green and Houston*, 1995 for a review). The physical mechanism responsible for deep-focus earthquakes remains elusive, as it is not known whether fluids [*Meade and Jeanloz*, 1991] play a role in deep-focus faulting or whether phase transitions [e.g., *Green and Burnley*, 1989] or rheological instabilities [*Hobbs and Ord*, 1988] are involved.

The 570 km deep March 9, 1994, M_w 7.6 Fiji and the 660 km deep June 9, 1994, M_w 8.2 Bolivia earthquakes (hereafter called Fiji and Bolivia earthquakes, Figure 1), are two of only 17 earthquakes in Harvard's Centroid Moment Tensor (CMT) catalog (1977-1994) deeper than 200 km and with M_w larger than 7. These two earthquakes are exceptional in that for the first time numerous digital broadband seismic instruments around the world and in the epicentral area provided on-scale recordings.

This paper presents an analysis of teleseismic broadband *P* waveforms recorded by IRIS and GEOSCOPE stations to model the rupture processes of the Fiji and Bolivia earthquakes. It is relatively straightforward to analyze *P* waves of deep earthquakes, because the surface reflections *pP* and *sP* arrive well separated from the direct *P* in the seismograms. Also, attenuation of *P* waves is relatively small and the details of the rupture process can be directly identified in the *P* wave train. We model arrival times and amplitudes of coherent subevents in *P* waveforms recorded at teleseismic distances and a wide range of azimuths to constrain the fault dimensions, direction of rupture and variations of focal mechanism during rupture. Waveform analyses are performed to estimate uncertainties in rupture extent and directivity as inferred from subevent arrival times.

Paper number 95GL02011
0094-8534/95/95GL-02011$03.00

Teleseismic *P* Waveforms

We utilize a total of 56 and 28 *P* waves of the Fiji and Bolivia events, respectively. Figure 2 shows representative waveforms. Some of the nodal stations show pronounced waveform differences resulting from small mechanism changes (e.g., PMSA, BKS, BAR for Fiji and RAR for Bolivia). For most of the azimuths and distances however, the considerable complexity in the *P* waveforms is coherent and due to rupture processes. The rupture of the Fiji earthquake consists of three major subevents (A, B and C in Figure 2) and has a total duration of approximately 12 s. The rupture of the Bolivia earthquake lasts about 40 s. A 10 s. low energy onset (labeled 'p') precedes the main moment release. Three peaks representative of the start, largest peak and end of the main rupture are labeled A, B, and C respectively.

Relative Arrival Times and Horizontal Directivity

Figure 3a and b show the arrival times of the subevents for both earthquakes (relative to the rupture onset times). The clear cosine dependence with azimuth indicates directivity, and is used to estimate relative time of occurrence and spatial offset between subevents ($time = t_0 - p{\cdot}X{\cdot}\cos(azimuth\text{-}\phi_0)$, where t_0 is the true relative time of occurrence, X is the spatial offset, p is the ray parameter of the wave and ϕ_0 is the directivity azimuth [e.g., *Chung and Kanamori*, 1980]). We estimate picking errors to be 0.5 s. for most stations and 1.0 s. for the nodal stations. These errors are reflected in the scatter in Figure 3. Some stations (e.g., PMSA and event C for PPT in Figure 3a) show much larger deviations probably resulting from subevent misidentifications. The solid curves in Figure 3 are the best cosine fits to the subevent arrival times. The fits for subevents A and B are not seriously affected by mispicks (for both earthquakes), but subevents C cannot be reliably located (dashed curves). The shaded curves and the error bars on the directivity azimuth are for cosine fits with a 10% larger misfit than the minimum misfit, and illustrate the relative accuracy with which each subevent can be located. Waveform analyses indicaté that the actual uncertainty in direction azimuth is probably about twice as large.

Figure 3c summarizes the relative locations of subevents A, B and C. The largest component of rupture of the Fiji earthquake, about 30 km in north to northwest direction, is between the onset and subevent B. Subevent A is located 10 km to the southeast of the hypocenter and indicates the possibility of a small bilateral directivity component. The total horizontal rupture is about 40 km, which is two thirds of the horizontal extent of aftershocks on the vertical plane [*Wiens et al.*, 1994]. Most of the directivity observed for the Bolivia earthquake occurs between the precursor 'p' and the initiation of the main moment release in east-north-east direction. The main subevents A, B and C display no more directivity than the order of magnitude smaller Fiji earthquake.

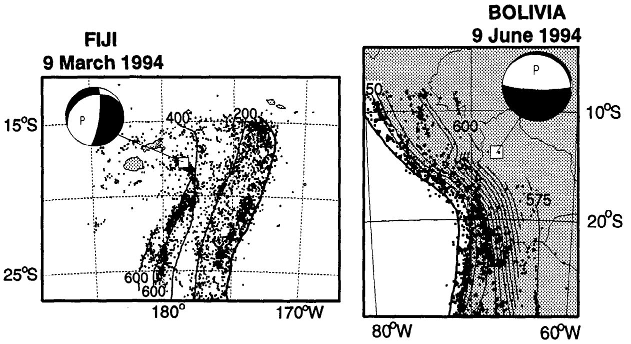

Figure 1. Maps showing the settings and major double couple Harvard CMT mechanisms of the Fiji and Bolivia main shocks. Locations of events with $m_b \geq 5$ (from the PDE catalog 1964-1994) and depth contours of the seismicity (from *Fischer and Jordan*, 1991 and *Cahill and Isacks*, 1992) illustrate the region of complex seismicity around the Fiji mainshock and the absence of seismicity near the Bolivia hypocenter.

Vertical Directivity from *P* and *pP* Durations

The relative times of subevents in the *P* waveforms are mainly sensitive to horizontal directivity. To estimate the amount of vertical directivity, we stacked *P* and *pP* waveforms recorded at TERRAscope stations in southern California (Figure 4). The difference in duration between Fiji *P* and *pP* stacks is about 3 seconds, which indicates the presence of a component of vertical rupture. Taking into account the relative effects of attenuation on the *P* and *pP* waveforms, we estimate that the vertical rupture is at most 40 km in up-dip direction. The *P* - *pP* duration difference for the Bolivia earthquake (Figure 4b) is small and is evidence for limited vertical directivity during rupture (< 20 km).

Subevent Amplitudes and Mechanism Changes

Variation of subevent amplitudes measured for stations at different distances and azimuths reflect mechanism changes during rupture. Figure 5 shows peak amplitudes, corrected for geometrical spreading, for each subevent plotted in a lower hemisphere projection. Focal mechanisms that best fit the amplitudes of the subevents are determined through a grid search over strike, dip and rake and represented by the shaded regions. For comparison the nodal planes of the Harvard point source mechanism are shown by dashed lines. The changes in strike and dip of the vertical nodal planes are better constrained than those of the horizontal planes, due to the distribution of stations.

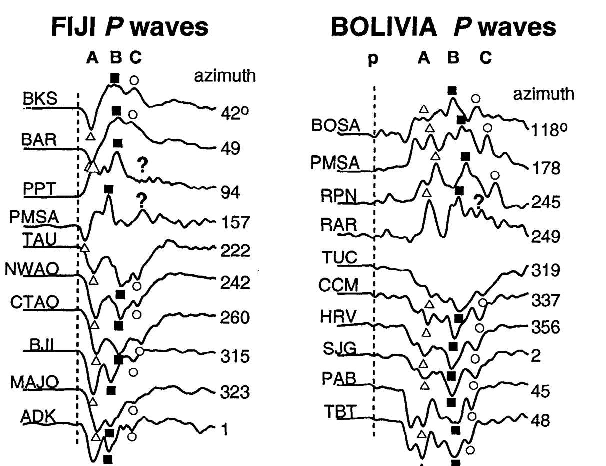

Figure 2. Representative *P*-displacements of the Fiji and Bolivia earthquakes. Several subevents (indicated by the letters p and A, B, C) can be correlated for most azimuths and distances. For some, mostly nodal, stations coherent subevents are hard to identify,. The *P* waveforms are lined up on the onset for Fiji and the first precursor (p) for Bolivia (dashed lines).

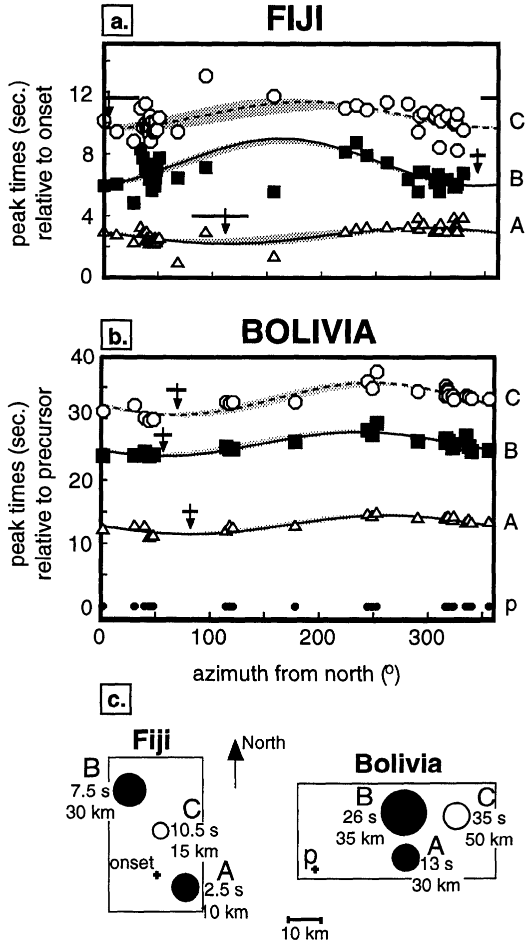

Figure 3. Arrival times of the subevents identified in Figure 2 as a function of azimuth indicate horizontal directivity in both the Fiji (**a.**) and Bolivia (**b.**)events. Times and directivity are relative to the onset (Fiji) or 'p' (Bolivia). Solid lines are a fit to the time picks assuming a unilateral rupture model (plotted for a single ray parameter). Arrows indicate the direction of rupture inferred from these models. The error bars and the shaded curves are for an increase in misfit of 10% relative to the optimum fit. The fits of events C are unreliable due to systematic picking errors (dashed lines). The rupture processes of the Fiji and Bolivia earthquakes as obtained from the time picks of subevents are schematically shown in **c**.

Both earthquakes have a vertical dip-slip mechanism with the compressional P-axis oriented generally in the down dip direction of the slab. Note that the negative polarity of Fiji's subevent A recorded by North American stations (e.g. BKS and BAR in Figure 2) and the negative polarity of Bolivia's precursor 'p' recorded at three South African stations (e.g. BOSA in Figure 2) require a slight mechanism change during rupture. Although the mechanism variations are resolvable, they are small and indicate little change in the slip direction, consistent with the small non-double couple component resolved by the Harvard CMT method.

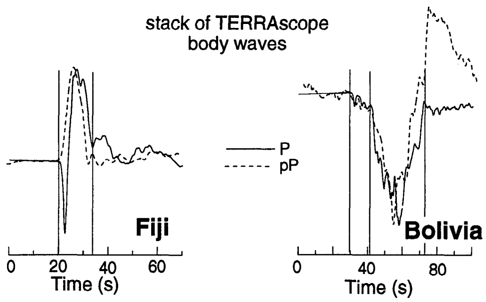

Figure 4. A comparison of the duration of *P* and *pP* waveforms from stacks of TERRAscope (southern California) stations to estimate vertical directivity. Limited vertical directivity is resolved for the Fiji earthquake, while no significant vertical rupture is apparent for Bolivia.

Waveform Analyses and Resolution

To estimate the reliability of the subevent picks, we perform several waveform analyses. We invert for mechanism and space-time distribution of moment release using a pulse-stripping technique developed by *Kikuchi and Kanamori* [1991]. We also perform forward modeling of the teleseismic *P* waveforms using various spatio-temporal distributions of subevents. Figure 6 illustrates how well the direction of rupture can be resolved using a line source. The variation of waveform misfit with rupture azimuth (in this case the azimuth of the line source) is also representative of more complex rupture models. The relative times, positions, moments and mechanisms of the subevents (based on the time pick analysis and a point source inversion) are fixed and constrained to lie in one of the CMT nodal planes.

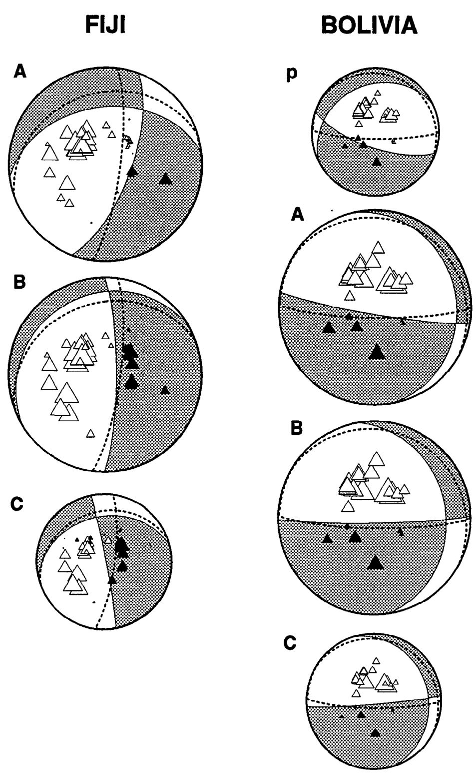

Figure 5. Best fitting focal mechanisms (shaded) and amplitudes of Fiji and Bolivia subevents. Open triangles represent amplitudes with negative polarity, solid triangles amplitudes with positive polarity. The size of the triangles is scaled according to the peak amplitudes, corrected for geometrical spreading. The Harvard CMT focal mechanism is shown with dashed lines. For both events we resolve small variations in mechanism.

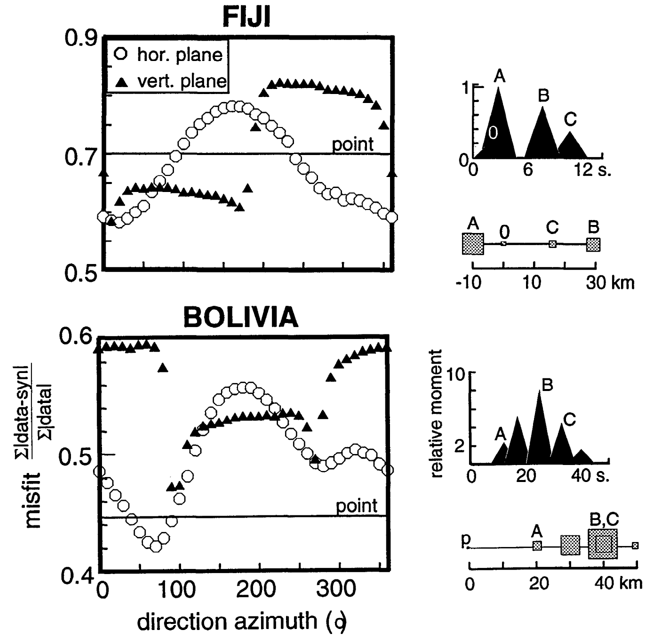

Figure 6. An illustration of the resolution of the direction of rupture obtained from various forward modeling analyses. Shown are waveform misfits as a function of the azimuth of a line source (left) with a fixed spatio-temporal distribution of subevents (right). The line sources are constrained to lie either within the horizontal nodal plane (white circles) or the vertical nodal plane (black triangles). For both the Fiji and the Bolivia earthquake the improvement over a point source (line) is small. We cannot determine the Fiji rupture plane using only P waveforms, as the horizontal and vertical planes give an equally good fit. There is a very slight preference for rupture along the horizontal plane in the Bolivia earthquake.

Fiji's subevents A and C must be located close to the hypocenter (within 10-15 km), while the main directivity is towards event B, located 30-40 km from the onset. A small counter-clockwise rotation of the strike of the vertical nodal plane is resolved. The misfit curve for the horizontal plane has a broad minimum. Rupture directions between 340° and 20° fit equally well (Figure 6). These directions include the solution we obtained from time picking. However waveforms can be fit as well with rupture along the vertical nodal plane in northward direction, so *P* wave analyses cannot resolve the fault plane ambiguity.

The Bolivia waveforms can be well modeled with a point source since most of the directivity is between the low amplitude precursor and the onset of main moment release. No significant change in fault mechanism was found. The preferred directivity is towards the east-north-east (50° to 90°, Figure 6) and probably on the horizontal plane, but it is poorly resolved. The total rupture length is approximately 40 to 60 km.

The waveform analyses suggest that the resolution of spatial moment release is limited due to the compactness of the rupture of the Fiji and Bolivia earthquakes both in space and time.

Discussion and Conclusions

Although the March 9, 1994, M_w 7.6 Fiji and the June 9, 1994, M_w 8.2 Bolivia events are much larger than most deep earthquakes recorded, their overall rupture characteristics are similar to those of many moderate size deep events [e.g., *Green*

Table 1. Rupture Parameters

	FIJI	BOLIVIA
CMT moment	$2.8 \cdot 10^{20}$ Nm	$3.0 \cdot 10^{21}$ Nm
duration	12 s	40 s
area of main moment release (S)	40x30 km^2	40x30 km^2
preferred rupture plane	"vertical"	"horizontal"
maximum rupture velocity	4-5 km/s	2-3 km/s
stress drop ($3.9 * M_0/S^{3/2}$)	26 MPa	283 MPa
average slip ($M_0/\mu S$)	2 m	20 m

and Houston, 1995]. Both earthquakes involve relatively short duration faulting, high stress drops (Table 1), and the compressional axes are aligned close to the down-dip slab directions. The main rupture characteristics given in Table 1 are in essence the same as those proposed in other studies [e.g., *McGuire et al.* 1994, *Kikuchi and Kanamori*, 1994, *Silver et al.*, 1995; and others in this issue]. As the ruptures of the Fiji and Bolivia earthquakes have limited spatial extent, differences in subevent locations between models are on the order of what can be resolved ($\pm$ 10 km) using teleseismic body waves.

Analyses of teleseismic *P* waves alone cannot resolve on which nodal plane the Fiji rupture occurred. However, the up-dip rupture of at most 40 km inferred from *P-pP* times is more readily accommodated on the steeply dipping nodal plane. This fault plane orientation is consistent with the alignment of aftershocks [*Wiens et al.*, 1994], a component of up-dip rupture resolved using local waveforms [*McGuire et al.*, 1994], and vertical lineations in the seismicity in Northern Tonga [*Giardini and Woodhouse*, 1984]. Assuming the vertical nodal plane is the actual fault plane, there is a small component of southward horizontal motion of the trench ward block, opposite to the direction of large scale shearing suggested by *Giardini and Woodhouse* [1984].

The east-north-east direction of rupture in the Bolivia earthquake and the small amount of vertical directivity are evidence for a shallowly dipping rupture plane. This is in agreement with the rupture direction and fault plane preferred by *Kikuchi and Kanamori* [1994] and *Silver et al.* [1995]. The northward slip of the earthquake is approximately perpendicular to the slip direction commonly observed in deep South American events, and may reflect deformation in response to a local bend in the slab inferred from seismicity at depths < 300 km [*Cahill and Isacks*, 1992].

The most notable differences between these two earthquakes are the difference in stress drop and rupture velocity (Table 1). These different rupture properties are perhaps characteristic of their tectonic settings (Figure 1). Numerous deep earthquakes occur in the Fiji-Tonga region, and most are relatively small. In contrast, the largest deep earthquakes occur in South America, and the Bolivia earthquake was located in a region with no previously known seismicity, and was followed by only one aftershock with M≥5 [*Myers et al.*, 1994]. Understanding rupture properties such as those resolved for the Fiji and Bolivia earthquakes in relation to their tectonic setting may provide important clues to identifying the physical mechanism underlying deep-focus faulting.

Acknowledgments. We thank H. Houston, T. Lay, and Q. Williams for helpful discussions and comments on the manuscript. We thank D. Giardini, D. Wiens and an anonymous reviewer for their constructive reviews IRIS and GEOSCOPE provided the high quality seismic data used in this study. This research was supported by the USGS under award number 1434-94-G2442 and by facilities support from the W. M. Keck Foundation. Contribution number 260 of the Institute of Tectonics.

References

Cahill T., and B. L. Isacks, Seismicity and shape of the subducted Nazca Plate, *J. Geophys. Res.*, *97*, 17,503-17,529, 1992.

Chung, W. and H. Kanamori, Variation of seismic source parameters and stress drops within a descending slab and its implications in plate mechanics, *Phys. Earth Planet. Int.*, *23*, 134-159, 1980.

Fischer, K.M., and T.H. Jordan, Seismic strain rate and deep slab deformation in Tonga, *J. Geophys. Res.*, *96*, 14,429-14,444, 1991.

Giardini, D. and J.H. Woodhouse, Deep seismicity and modes of deformation in the Tonga subduction zone, *Nature*, *307*, 505-509, 1984.

Green II, H.W., and P.C. Burnley, A new self-organizing mechanism for deep-focus earthquakes, *Nature*, *341*, 733-737, 1989.

Green II, H.W., and H. Houston, The mechanics of deep earthquakes, *Annu. Rev. Earth. Planet. Sci.*, *23*, 169-213, 1995.

Hobbs, B.E. and A. Ord, Plastic instabilities: implications for the origin of intermediate and deep focus earthquakes, *J. Geophys. Res.*, *93*, 10,521-10,540, 1988.

Kikuchi, M. and H. Kanamori, The mechanism of the deep Bolivia earthquake of June 9, 1994, *Geophys. Res. Lett.*, *21*, 2341-2344, 1994.

Kikuchi, M. and H. Kanamori, Inversion of complex body waves 3., *Bull. Seismol. Soc. Am.*, *81*, 2335-2350, 1991.

McGuire, J.J, D.A. Wiens, P.J. Shore, M.G. Bevis, K. Draunidalo, G. Prasad, and S.P. Helu, Rupture properties of the March 9 deep Tonga earthquake and its aftershocks, *Eos Trans. Am. Geophys. Un.*, *75*, 466, 1994.

Meade, C. and R. Jeanloz, Deep-focus earthquakes and recycling of water into the Earth's mantle, *Science*, *252*, 68-72, 1991.

Myers, S.C., T.C. Wallace, S.L. Beck, P.G. Silver, G. Zandt, J. Vandecar, and E. Minaya, Implications of spatial and temporal development of the aftershock sequence for the M_W 8.3 June 9, 1994 deep Bolivian earthquake, *submitted to Geophys. Res. Lett.*, 1994.

Silver, P.G., S.L. Beck, T.C. Wallace, C. Meade, S.C. Myers, D.E. James, R. Kuehnel, The rupture characteristics of the great, deep Bolivian earthquake of 1994, and the physical mechanism of deep-focus earthquakes, *Science*, *in press*, 1995.

Wiens, D.A., J.J McGuire, P.J. Shore, M.G. Bevis, K. Draunidalo, G. Prasad, and S.P. Helu, A deep earthquake aftershock sequence and implications for the rupture mechanism of deep earthquakes, *Nature*, *372*, 540-543, 1994.

S. Goes and J. Ritsema, Institute of Tectonics and W.M. Keck Seismological Laboratory, University of California, Santa Cruz, CA 95064 (e-mail: saskia@earthsci.ucsc.edu, jeroen@earthsci.ucsc.edu)

(Received November 7, 1994; revised April 18, 1995;
accepted May 30, 1995.)